Crowded and warmer: unequal dengue risk at high spatial resolution across a megacity of India

Victoria Romeo-Aznar[1*], Mauricio Santos-Vega[2], Olivier Telle[3], Richard Paul[4] and Mercedes Pascual[5,6]

1 Departamento de Ecología, Genética y Evolución, and Instituto IEGEBA (CONICET-UBA), Facultad de Ciencias Exactas y Naturales, Universidad de Buenos Aires, Ciudad Universitaria, Pabellón 2, C1428EHA, Buenos Aires, Argentina

2 Grupo de investigación en Biología Matemática y Computacional (BIOMAC), Departamento de Ingeniería Biomédica, Universidad de los Andes, Bogotá, Colombia

3 Géographie-cités, Université´ Paris-1 Panthéon-Sorbonne, Paris, France

4 Ecology and Emergence of Arthropod-borne Pathogens unit, Institut Pasteur, Université Paris-Cité, Centre National de Recherche Scientifique (CNRS) UMR 2000, Institut National de Recherche pour l'Agriculture, l'Alimentation et l'Environnement (INRAE) USC 1510, 75015 Paris, France

5 Department of Ecology and Evolution, University of Chicago, Chicago, IL, USA

6 The Santa Fe Institute, Santa Fe, NM, USA

*** Corresponding author**

Victoria Romeo-Aznar vromeoaznar@gmail.com

Abstract

The role of climate factors on transmission of mosquito-borne infections within urban landscapes must be considered in the context of the pronounced spatial heterogeneity of such environments. Socio-demographic and environmental variation challenge control efforts for emergent arboviruses, a major class of pathogens responsible for dengue, Zika and chikungunya, transmitted via the urban mosquito *Aedes aegypti*. We address at high resolution, the spatial heterogeneity of dengue transmission risk in the megacity of Delhi, India, as a function of both temperature and the carrying-capacity of the human environment for the mosquito. Based on previous results predicting maximum mosquitoes per human for different socio-economic typologies, and on remote sensing temperature data, we produce a map of the reproductive number of the disease at a resolution of 250m by 250m. We focus on dengue risk hotspots during inter-epidemic periods, places where chains of transmission can persist for longer. We assess the resulting high-resolution risk map of dengue with reported cases for three consecutive winters. We find that both temperature and vector carrying-capacity per human co-vary in space because of their respective dependence on population density. The synergistic action of these two factors results in larger variation of dengue's reproductive number than when considered separately, with poor and dense locations experiencing the warmest conditions and becoming the most likely reservoirs off-season. The location of observed winter cases is accurately predicted for different risk threshold criteria. Results underscore the inequity of risk across a complex urban landscape, whereby individuals in dense poor neighborhoods face the compounded effect of higher temperatures and mosquito carrying capacity. Targeting chains of transmission in inter-epidemic periods at these locations should be a priority of control efforts. A better mapping is needed of the interplay between climate factors that are dominant determinants of the seasonality of vector-borne infections and the socio-economic conditions behind unequal exposure.

Introduction

Climate change, globalization, and rapid population growth are accelerating the spread of established pathogens and facilitating the emergence of novel ones, modifying geographical limits and environmental suitability for transmission (1,2). Spatial resolutions finer than those of countries and cities are becoming critical to understand the epidemiology of vector-borne infections, including those transmitted by the widespread urban mosquito *Ae. aegypti* and caused by arboviruses such as dengue and Zika (3–5). Although traditional “well-mixed” mathematical models provide a foundation for epidemiological theory (6,7), the increasing availability of fine-scale data has underscored the importance of explicitly considering the spatial dimension (e.g. 8,9). Consideration of highly-resolved spatial scales is essential to the prediction of transmission risk and efficiency of control efforts in urban landscapes where human density and mosquito abundance can vary widely.

The persistence of dengue virus transmission in urban settings is challenging to control efforts given the pronounced heterogeneity in environmental, demographic and socio-economic conditions. Because humans effectively generate breeding sites for *Ae. aegypti* in the form of a variety of small water containers (10), vector abundance within cities depends on population density and infrastructure (11). The generation of water containers can vary spatially also as a function of socio-economic conditions, especially in developing countries where unplanned urbanization and limited resources leave a part of the population without regular or continuous access to pipe water and garbage collection.

Temperature, another important determinant of vector-borne transmission, can also vary within cities because of the urban heat island effect (UHI). Temperature influences the demographic parameters of mosquitoes, as well as transmission parameters, ultimately determining vectorial capacity (12–14). Importantly, land surface modifications make urban areas warmer than their surrounding peri-urban or rural landscapes (3). Although the local cause of the UHI can vary, several high-resolution remote sensing studies have shown that the intensity of UHI can correlate positively with human population density (15–17). Usually, these temperature differences are larger at night than during the day and are more noticeable during summer and winter (18,19). A better understanding of how UHI contributes to dengue transmission hotspots would be invaluable to optimize deployment of mosquito control resources across the scale of a metropolis. Thus, high-resolution datasets allowing translation of temperature heterogeneity into transmission risk especially outside the epidemic season could help us locate environmental niches where mosquitoes survive and breed, enabling viral persistence. Hypothetically, targeting such localized reservoirs could interrupt or minimize chains of transmission across seasons.

Here we examine dengue transmission risk at a high resolution (250m by 250m) in the megacity of Delhi, India. By considering the basic reproduction number, we explore the interplay of temperature in winter with the vector's carrying capacity in relation to human population density. We show that these two environmental factors act synergistically, producing a larger variation in local disease risk than when considered separately. Case reports for three winters are used to evaluate our risk map. Results underscore the inequity of risk across a complex urban landscape: individuals in dense poor neighborhoods face the compounded effect of warmer temperatures. We then discuss this result in the greater context of global climate change.

Results

We focus on the basic reproduction number, $R0$, one of the most fundamental quantities in epidemiology measuring the average number of secondary infections produced by one single infection in a totally susceptible population. Although the precise form of $R0$ depends on the model, its general expression for mosquito-borne diseases (with a single host and vector) can be typically written in such a way to separate the respective effect of two key factors, namely temperature and the maximum number of mosquitoes per human the environment can support, hereafter referred to as the vector's carrying capacity. Specifically, *R*0 can be decomposed into the product of two terms: a function of temperature (that impacts biological parameters of the mosquito and the pathogen within the mosquito), and the ratio of the vector's carrying capacity (*V*) to the human population (*N*) (Methods). We can thus write $R0 = f(T)\sqrt{\frac{V}{N}}$, an expression decomposing the effects of climate and socio-economic conditions.

These two variables in the general expression for *R*0 are spatially heterogeneous within the city of Delhi in the winter season (Fig. 1A). Spatial temperature (*T*) varies about five degrees Celsius (mean *T*=18.6 °C) and the ratio of the vector's carrying capacity to the human population (*V*/*N*) shows values ranging from zero to 1.5 (mean *V*/*N*=0.4). Importantly, both quantities, *T* and *V*/*N*, can vary as a function of human density and therefore share a common source of spatial variation. To first address this dependence for *V*/*N*, we note that mosquito recruitment in urban landscapes is intrinsically related to human activity. The map for *V*/*N* specifically relies on the previously inferred dependence of the vector carrying capacity on human density in (20) (Fig. 1B, see Methods). The shape of the function was shown to vary for different socio-economic categories (low, medium and high) as defined in (20,21). In particular, 87% of the spatial units correspond to socio-economic conditions for which *V*/*N* increases with population density, with locations that exhibit the most deprived conditions experiencing the fastest increment. Second, for winter temperature, we find here that values, at the same high resolution of interest, are also affected by human density. Although the least dense areas show the highest variability, those most populated tend to be systematically warmer (Fig. 1C). Together, these two patterns suggest the potential synergy of the two environmental variables on dengue risk across the city. In particular, population density would drive the spatial co-localization of elevated winter temperature and vector's carrying capacity.

Fig. 1. Temperature (*T*) and vector carrying capacity per human (*V*/*N*) in Delhi. A Maps

for a spatial resolution of 250m by 250m for temperature (November night-time) and *V*/*N* in the city of Delhi. **B** Vector carrying capacity (maximum number of mosquitoes per human) as a function of population density for deprived (triangles), medium (circles) and rich (dots) typologies. **C** Boxplot of November night-time temperature as a function of population density (boxes illustrate, as is standard, the median with the 25th and 75th percentiles, and the dotted lines indicate the extremes of the distribution).

To address this hypothesis, we examine first the separate effect of each of the two variables and then their joint influence on the spatial variability of *R*0. Frequency distributions in the form of histograms show that both *T* and *V*/*N* generate broad ranges in *R*0's spatial variability. Compared to the spatial average of *R*0 (about 0.4), consideration of temperature introduces a variation of up to 40% (Fig. 2A) and consideration of *V*/*N* of up to 75% (Fig. 2B). The associated maps exhibit variation that would be absent not only under constant temperatures as expected, but also under the common assumption of a linear increase of vectors with humans in standard coupled vector-human mathematical models (Fig. 2A, B and C). Importantly, when both factors are considered together, the range of *R*0 is larger than when they are considered separately, with many more units at the two extremes of high and low risk conditions (Fig. 2C). In particular, units that do not exhibit a high dengue risk under either factor alone, can do so when their joint effect is considered together (Fig. 2D). Thus, comparison of the maps indicates that *T* and *V*/*N* act synergistically in a considerable part of the city.

Fig. 2. The effect on the basic reproductive number *R*0 of temperature (*T*) and vector carrying capacity per human (*V*/*N*). Maps and histograms of local *R*0 at 250 m by 250 m spatial resolution for: **(A)** local temperature with spatially averaged *V*/*N*, **(B)** local *V*/*N* with spatially averaged temperature and, **(C)** local temperature and *V*/*N*. Blue, aqua green and red colors represent respectively a low (*R*0 < 0.3), medium (0.3 < *R*0 < 0.55) and high (*R*0 > 0.55) risk of local dengue transmission. (**D)** Percentage of units at high risk for different risk threshold values, computed for: local *T* with spatially averaged *V*/*N* (green dots), local *V*/*N* with spatially averaged *T* (red dots), and both local *T* and *V*/*N* (black dots).

To examine whether the generated risk map has predictive value, we rely on surveillance data over three winter seasons for reported dengue cases at high spatial resolution (Methods). First, we establish a threshold *R*0* to classify spatial units at risk of dengue transmission when $R0$ is above this value ($R0_u > R0^*$, u=1,2,.... U, where U is the total number of units). Since small values of $R0^*$ imply a higher number of units at risk, we expect the percent of "hits", defined as units whose observed cases surpass the threshold, to decrease with increasing $R0^*$. However, a high number of hits is not necessarily informative. We can illustrate this by the trivial extreme of $R0^*=0$, for which we would obtain a 100% trivial success rate because the whole city would be at risk. Thus, to evaluate the $R0$ criterion, we compute as a baseline the probability of the number of realized hits under the assumption of a random spatial distribution of infected units (for a given threshold). We specifically compute the *p-value* of a binomial process:

$$p-value=\sum_{i=K}^{U_f}\binom{U_f}{i}p^i(1-p)^{U_f-i}$$

where the number of trials is the number of infected units U_f, the number of units with cases classified at risk is the number of hits K, and the probability that a risk unit is randomly infected is $p=UR/U$, for the number of risk units UR. We find that the *p-value* is consistently below 0.05 as $R0^*$ increases, leading us to reject a random distribution of cases relative to our risk map. (A *p-value* larger than 0.05 is only obtained when $R0^*$ equals the 97.5th quantile, that is when 2.5% of the units are classified at high risk).

Because population density underlies both components of $R0$, we can further ask whether considering a threshold defined directly on the basis of local human density would also be informative. We repeat the calculation of a binomial probability now with a minimum population density threshold as an indicator of dengue transmission during the winter season. We find that this condition works as well as one defined on the basis of $R0$ as an indicator of winter hotspots (see Fig. 3).

Fig. 3. Performance of risk maps for the prediction of dengue cases in winter (at a resolution of 250 m by 250 m). The *p-value* is computed from a binomial process for different risk thresholds. The threshold values are defined by the percent of units at risk (quantiles), for the criterion based on either $R0$ (black dashes) or population density (N) (red

circles).

Discussion

The spatial distributions of the two dengue drivers taken together, for temperature and vector carrying capacity to human ratio, are here shown to produce important variability in local suitability for virus transmission at high resolution within the city. Although the influence of these drivers could be expected, their joint action reflects a common underlying influence of population density, which proves critical for the localization of winter hotspots. Identification of such hotspots will be invaluable for interrupting the chain of transmission during the low season when it should be most vulnerable to intervention.

The synergistic action of the two drivers especially affects the least developed areas of the city, with 70% of the winter cases reported from within socio-economic units classified as deprived, and only 22% and 8%, from medium and rich typologies respectively. Deprived units are typically densely populated with only a few green areas, which can favor the UHI effect. In addition, the number of vectors per human is higher in poor areas of the city, where one can expect a higher production of breeding containers (10). This socio-economic disparity in dengue suitability is also clear in our risk map, which yields a higher percentage of risk units in the deprived typology as the threshold $R0^*$ increases (Fig. S1).

The location of reported cases over three winter periods validates the high-resolution risk map obtained here when compared to the random distribution of infections across units. Although the values of $R0$ obtained for our map remain below one, this does not necessarily imply the absence of transmission (22,23). The commonly used threshold of $R0$=1 assesses the risk of an outbreak from a purely deterministic perspective. Although such an outbreak is not expected in Delhi during the off-season and transmission in small areas is inherently stochastic, higher values of $R0$ even below one, should indicate higher transmission suitability, and therefore a higher chance of persistence of transmission chains off-season.

Because human density influences local vector carrying capacity and temperature, this quantity can also be used effectively as an indicator of dengue transmission risk in winter. As a purely statistical indicator, the associated threshold can be less informative, however, than a more mechanistic and direct understanding of how population density ultimately impacts risk (24–26).

A limitation of our results is the reliance on a single detailed remote sensing image. The pattern of increasing temperature with density should, however, hold more generally as it has been reported by other studies (15,16).

Direct measures of mosquito abundance across the urban landscape would be valuable but extremely challenging in practice, especially at fine scales (27). Mathematical models of coupled vector-human transmission commonly assume a constant vector-to-human ratio (28). This implicit assumption implies a constant risk landscape across the city in terms of V/N and, therefore, precludes the variation in risk described here. We have relied, for our risk map, on an indirect estimate of maximum mosquito numbers per human (20). Interestingly, the predictive power of the $R0$ threshold provides support for this indirect estimation of V/N.

The challenges posed by climate change require a robust and holistic approach to understanding infectious disease dynamics (23). Understanding climate change effects on infectious disease transmission remains a crucial gap within urban landscapes at sufficiently high spatial resolutions, including potential synergies with various demographic and socio-economic drivers. We have shown that the fine-scale interaction of temperature and socio-economic conditions (related to vector production) amplifies local dengue transmission suitability. Both these factors are sensitive to climate change directly and indirectly. Warmer winter temperatures where cold temperatures limit transmission can favor persistence of mosquito populations outside the epidemic season. Climate change can also favor breeding site production, as climate instability in the form of extreme events can contribute to poverty and overcrowding as the result of enhanced and unplanned human migration (29). Although our findings are for dengue in the megacity of Delhi, we expect the described synergistic effect of temperature and mosquito carrying capacity to apply more broadly to other urban landscapes and other climate-sensitive infections, especially in developing countries with seasonal transmission.

Methods and Materials

Expression of the basic reproductive number as a function of temperature and vector carrying capacity per human.

The basic reproductive number gives the average number of secondary infections that would result from introducing a single infective individual into an entirely susceptible population. Calculation of *R*0 for dengue infection involves a two-step process: host to vector, then vector back to host (or vice versa). To illustrate this process, we rely on the following standard equations for the infectious classes in coupled vector-human models:

$$dI/dt = a P_{MH} Z S/N - (\mu_H + \gamma) I \qquad (1a)$$

$$dZ/dt = a P_{HM} W I/N - \mu_M Z \qquad (1b)$$

where *W*, *Z* and *M* (for mosquitoes), and *S*, *I* and *N* (for humans), denote susceptible, infectious and total populations, respectively. Parameter a denotes the biting rate, P_{MH} (for a human) and P_{HM} (for a mosquito) are the respective probabilities that an infectious bite results in an infection, γ is the recovery rate of infected humans, and μ_H and μ_M the respective mortality rates for humans and mosquitoes.

Let $R0_{MH}$ be the number of hosts directly infected by the introduction of a single infective vector into an entirely susceptible host population. Similarly, let $R0_{HM}$ denote the number of vectors that become directly infected upon the introduction of a single infectious host into an entirely susceptible vector population. When the host population is entirely susceptible (I=0 and then S=N), the transmission rate from the vector population to the host population is given by $a \cdot P_{MH} \cdot Z$. Thus, the transmission rate per infective vector equals $a \cdot P_{MH}$ (eq. 1a). Since infective vectors live for an average of 1/μ_M time units, a single infective vector will give rise to $R0_{MH} = a \cdot P_{MH} / \mu_M$ infective hosts. Employing a similar argument for an entirely susceptible vector population (Z=0 and thus W=M), we obtain (eq. 1b) $R0_{HM} = \left(a \cdot P_{HM} / (\mu_M + \gamma)\right) \cdot (M/N)$. Therefore, over the entire transmission cycle we obtain the following expression,

$$R0 = \sqrt{R0_{HM} \cdot R0_{MH}} = \sqrt{\frac{a^2 P_{HM} P_{MH}}{\mu_M(\gamma + \mu_H)}} \sqrt{\frac{M}{N}} = h(T) \sqrt{\frac{M}{N}} \qquad (2)$$

(e.g. (30)). We can decompose this expression into two main factors: one that depends on demographic and biological parameters which are constant or depend on temperature ($h(T)$, where T is temperature), and another that is the ratio between mosquito and human numbers.

Because the developmental life cycle of *Ae. aegypti* is complex, coupled mosquito-human models commonly assume that the total abundance of mosquitoes follows logistic growth, with for example an equation of the form

$$dM/dt = \lambda M\left(1 - M/K\right) \quad (3)$$

where λ represents the number of offspring per adult female per unit time, and, *K,* the carrying capacity supported by the environment. By making a quasi-stationary assumption whereby the population dynamics of the vector equilibrates quickly to temporal variation, we can consider that M ~ K (by equating eq. (3) to zero). Variations of this expression for mosquito abundance are of course obtained depending on model details. For example, (30,31) proposes that $dM/dt = EFD \cdot pEA \cdot MDR \cdot \mu_M{}^{-1} \cdot M \cdot \left(1 - M/K\right) - \mu_M \cdot M$ (an expression obtained by adding equations (1), (2) and (3) for susceptible, exposed and infectious mosquitoes populations in the original article), and therefore

$$M \quad \left(1 - \mu_M{}^2 / \left(EFD \cdot pEA \cdot MDR\right)\right) \cdot K$$

where *EFD* is the number of eggs laid per female per day, *pEA* is the probability of mosquito egg-to-adult survival, and *MDR* is the mosquito egg-to-adult development rate. Another example is found in (20) where

$$M \quad \left(\lambda / \mu_M\right) \cdot K$$

In short, models in which the differential equation for mosquito abundance follows a form in the family of logistic functions (eq. (3)), produce generically the form $M \quad g(T) \cdot K$, where the particular expression of the function *g*(*T*) depends on the model.

Here, we specifically used the following differential equation for adult mosquitos

$$\frac{dM}{dt} = EFD \cdot pEA \cdot M \cdot \left(1 - \frac{M}{K}\right) - \mu_M \cdot M \quad (4)$$

Then, by introducing the value of *M* obtained from equating the left-hand side of this equation to zero into the expression in eq. (2), we specifically obtain

$$R0=\sqrt{\frac{a^2 P_{HM} P_{MH}}{\mu_M(\gamma+\mu_H)}}\sqrt{\frac{M}{N}}=\sqrt{\frac{a^2 P_{HM} P_{MH}}{\mu_M(\gamma+\mu_H)}}\sqrt{1-\frac{\mu_M}{EFD\, pEA}}\sqrt{\frac{K}{N}}=h(T)g(T)\sqrt{\frac{K}{N}}=f(T)\sqrt{\frac{K}{N}}$$

(5)

The values of the parameters of *f*(*T*) and their dependence with temperature are given in Table 1. We emphasize that although we illustrate the risk maps for this model and therefore this specific form of *f(T)*, the results should generalize to other models.

The carrying capacity as a function of the human population per spatial unit is computed with the curves inferred in (20). We summarize here the basic approach. For *Ae. aegypti*, it is reasonable to consider that *K* depends on *N*, or *K*=*K*(N), since humans generate the breeding sites for the mosquito. We can expect that this production of breeding sites and therefore the shape of the *K*(*N*) function, depend in turn on socio-economic conditions of the local human population. Because it remains extremely challenging to sample and quantify mosquito numbers, we rely on the results obtained in (20) where mosquito numbers were inferred from human population density. Importantly, *K*(N) was shown to vary with socio-economic conditions on the basis of the typologies classified in (21), with $K \propto N^2$ and $K \propto N^{1.24}$ for typologies denoted respectively as deprived and intermediate, and a non-monotonic, increasing and then decreasing, behavior for those denoted as rich (see Fig. 1B).

symbol	description	formula	parameters value
a	biting rate (days^{-1})	$c \cdot T \cdot (T-T_{min}) \cdot \sqrt{T_{max}-T}$	(32)
EFD	rate of eggs laid per female (days^{-1})	$c \cdot T \cdot (T-T_{min}) \cdot \sqrt{T_{max}-T}$	(32)

pEA	probability of mosquito egg-to-adult survival	$c \cdot (T - T_{min}) \cdot (T_{max} - T)$	(32)
μ_M	mosquito mortality (days^{-1})	const.	0.09 (33)
P_{HM}	probability virus transmission from human to mosquito	const.	0.8
P_{MH}	probability virus transmission from mosquito to human	$c \cdot T \cdot (T - T_{min}) \cdot \sqrt{T_{max} - T}$	c=0.00092 T_{min}=13 T_{max}=33
γ	human recovery rate (days^{-1})	const.	1/7 (34)
μ_H	human mortality (days^{-1})	const.	1/(60.365) (35)

TABLE 1. Model parameter specifications. Values without references indicate that have been determined for this article (see Fig S1).

Temperature data from remote sensing

Satellite brightness temperature was retrieved from LANDSAT 8 TIRS (band 10). The thermal image was taken on November 15, 2013 at around 5:00 AM. Land surface temperature was computed by the methods of [Walawender 2014] (by incorporating the correction equations for land surface emissivity and atmospheric bias). Surface temperatures were obtained at a 38 m scale and then aggregated to the 250 m by 250 m spatial resolution (see details on (36)).

Dengue cases for the winter season

The dengue cases were geo-localized for the winter seasons from 2013 to 2015. These are the seasons for which dengue cases were reported in winter for the first time. Dengue cases were confirmed for the presence of IgM antibodies against DENV by MAC ELISA using a kit prepared by the National Institute of Virology, Pune, India as an integral part of the National Vector Borne Disease Control Programme.

These confirmed cases were geo-coded with QGIS (36).

Ethics Statement

Written consent to participate in the study was obtained from all participants and ethical approval was granted by the ethics committees of the Indian Council for Medical Research, India (N° TDR/587/2012-ECD-11, 10 December 2012) and Institut Pasteur, France (N° 2011–20, 29 April 2011). If human subjects were not adult, a parent or guardian of the child provided written informed consent on their behalf. Patient data were anonymized.

Acknowledgments

We are grateful for the support of a collaborative grant from the National Science Foundation's Division of Mathematical Sciences and the National Institutes of Health (no. 1761612: Collaborative Research: Urban Vector-Borne Disease Transmission Demands Advances in Spatiotemporal Statistical Inference to M.P. and E. Ionides). During the initial part of this work, V.R-A. was jointly supported by this grant and by the Mansueto Institute for Urban Innovation through a Mansueto Institute Postdoctoral Fellowship. MP also thanks the FACCTS program of the University of Chicago (France and Chicago Collaborating in the Sciences), which made possible the initial collaboration of the co-authors, and MSV, the support of the International Development Research Centre (IDRC) (no. 109848)

References

1. Liyanage, P., Tozan, Y., Overgaard, H.J., Tissera, H.A. and Rocklöv, J. Effect of El Niño–Southern Oscillation and local weather on Aedes vector activity from 2010 to 2018 in Kalutara district, Sri Lanka: a two-stage hierarchical analysis. The Lancet Planetary Health [Internet]. 2022 Jul 1 [cited 2023 Mar 30];6(7):e577–85. Available from: http://dx.doi.org/10.1016/S2542-5196(22)00143-7

2. Lowe R, Lee SA, O'Reilly KM, Brady OJ, Bastos L, Carrasco-Escobar G, et al. Combined effects of hydrometeorological hazards and urbanisation on dengue risk in Brazil: a spatiotemporal modelling study. Lancet Planet Health [Internet]. 2021 Apr;5(4):e209–19. Available from: http://dx.doi.org/10.1016/S2542-5196(20)30292-8

3. Misslin R, Telle O, Daudé E, Vaguet A, Paul RE. Urban climate versus global climate change-what makes the difference for dengue? Ann N Y Acad Sci [Internet]. 2016 Oct;1382(1):56–72. Available from: http://dx.doi.org/10.1111/nyas.13084

4. Santos-Vega M, Bouma MJ, Kohli V, Pascual M. Population Density, Climate Variables and Poverty Synergistically Structure Spatial Risk in Urban Malaria in India. PLoS Negl

Trop Dis [Internet]. 2016 Dec;10(12):e0005155. Available from: http://dx.doi.org/10.1371/journal.pntd.0005155

5. Lourenço J, Maia de Lima M, Faria NR, Walker A, Kraemer MU, Villabona-Arenas CJ, et al. Epidemiological and ecological determinants of Zika virus transmission in an urban setting. Elife [Internet]. 2017 Sep 9;6. Available from: http://dx.doi.org/10.7554/eLife.29820

6. Mollison D, Denis M. Epidemic Models: Their Structure and Relation to Data [Internet]. Cambridge University Press; 1995. 424 p. Available from: https://play.google.com/store/books/details?id=MZRkdfOByIYC

7. Fofana AM, Hurford A. Mechanistic movement models to understand epidemic spread. Philos Trans R Soc Lond B Biol Sci [Internet]. 2017 May 5;372(1719). Available from: http://dx.doi.org/10.1098/rstb.2016.0086

8. Riley S, Eames K, Isham V, Mollison D, Trapman P. Five challenges for spatial epidemic models [Internet]. Vol. 10, Epidemics. 2015. p. 68–71. Available from: http://dx.doi.org/10.1016/j.epidem.2014.07.001

9. Moss R, Naghizade E, Tomko M, Geard N. What can urban mobility data reveal about the spatial distribution of infection in a single city? BMC Public Health [Internet]. 2019 May 29;19(1):656. Available from: http://dx.doi.org/10.1186/s12889-019-6968-x

10. Vikram K, Nagpal BN, Pande V. Comparison of Ae. aegypti breeding in localities of different socio-economic groups of Delhi, India. Journal of Mosquito … [Internet]. 2015; Available from: http://www.dipterajournal.com/pdf/2015/vol2issue3/PartB/2-2-45-618.pdf

11. Kolimenakis A, Heinz S, Wilson ML, Winkler V, Yakob L, Michaelakis A, et al. The role of urbanisation in the spread of Aedes mosquitoes and the diseases they transmit-A systematic review. PLoS Negl Trop Dis [Internet]. 2021 Sep;15(9):e0009631. Available from: http://dx.doi.org/10.1371/journal.pntd.0009631

12. Liu-Helmersson J, Stenlund H, Wilder-Smith A, Rocklöv J. Vectorial capacity of Aedes aegypti: effects of temperature and implications for global dengue epidemic potential. PLoS One [Internet]. 2014 Mar 6;9(3):e89783. Available from: http://dx.doi.org/10.1371/journal.pone.0089783

13. Mordecai EA, Caldwell JM, Grossman MK, Lippi CA, Johnson LR, Neira M, et al. Thermal biology of mosquito-borne disease. Ecol Lett [Internet]. 2019 Oct;22(10):1690–708. Available from: http://dx.doi.org/10.1111/ele.13335

14. Lahondère C, Bonizzoni M. Thermal biology of invasive Aedes mosquitoes in the context of climate change. Curr Opin Insect Sci [Internet]. 2022 Jun;51:100920. Available from: http://dx.doi.org/10.1016/j.cois.2022.100920

15. Mallick J, Rahman A. Impact of population density on the surface temperature and micro-climate of Delhi. Curr Sci [Internet]. 2012;102(12):1708–13. Available from: http://www.jstor.org/stable/24084829

16. Li L, Tan Y, Ying S, Yu Z, Li Z, Lan H. Impact of land cover and population density on land surface temperature: case study in Wuhan, China. JARS [Internet]. 2014 Mar [cited 2023 Mar 31];8(1):084993. Available from: https://www.spiedigitallibrary.org/journals/Journal-of-Applied-Remote-Sensing/volume-8/issue-1/084993/Impact-of-land-cover-and-population-density-on-land-surface/10.1117/1.JRS.8.084993.short

17. Jaber SM. Is there a relationship between human population distribution and land surface temperature? Global perspective in areas with different climatic classifications. Remote Sensing Applications: Society and Environment [Internet]. 2020 Nov 1;20:100435. Available from: https://www.sciencedirect.com/science/article/pii/S2352938520303062

18. Oke TR. The energetic basis of the urban heat island. Quart J Roy Meteor Soc [Internet]. 1982; Available from: https://www.patarnott.com/pdf/Oake1982_UHI.pdf

19. Phelan PE, Kaloush K, Miner M, Golden J, Phelan B, Silva H, et al. Urban Heat Island: Mechanisms, Implications, and Possible Remedies. Annu Rev Environ Resour [Internet]. 2015 Nov 4;40(1):285–307. Available from: https://doi.org/10.1146/annurev-environ-102014-021155

20. Romeo-Aznar V, Paul R, Telle O, Pascual M. Mosquito-borne transmission in urban landscapes: the missing link between vector abundance and human density. Proc Biol Sci [Internet]. 2018 Aug 15;285(1884). Available from: http://dx.doi.org/10.1098/rspb.2018.0826

21. Telle O, Vaguet A, Yadav NK, Lefebvre B, Daudé E, Paul RE, et al. The Spread of Dengue in an Endemic Urban Milieu–The Case of Delhi, India. PLoS One [Internet]. 2016 Jan 25 [cited 2023 Mar 31];11(1):e0146539. Available from: https://journals.plos.org/plosone/article/file?id=10.1371/journal.pone.0146539&type=printable

22. Antia R, Regoes RR, Koella JC, Bergstrom CT. The role of evolution in the emergence of infectious diseases. Nature [Internet]. 2003 Dec 11;426(6967):658–61. Available from: http://dx.doi.org/10.1038/nature02104

23. Heffernan C. Climate change and multiple emerging infectious diseases. Vet J [Internet]. 2018 Apr;234:43–7. Available from: http://dx.doi.org/10.1016/j.tvjl.2017.12.021

24. Baker RE, Peña JM, Jayamohan J, Jérusalem A. Mechanistic models versus machine learning, a fight worth fighting for the biological community? Biol Lett [Internet]. 2018 May;14(5). Available from: http://dx.doi.org/10.1098/rsbl.2017.0660

25. Kandula S, Yamana T, Pei S, Yang W, Morita H, Shaman J. Evaluation of mechanistic and statistical methods in forecasting influenza-like illness. J R Soc Interface [Internet]. 2018 Jul;15(144). Available from: http://dx.doi.org/10.1098/rsif.2018.0174

26. Holmdahl I, Buckee C. Wrong but Useful - What Covid-19 Epidemiologic Models Can and Cannot Tell Us. N Engl J Med [Internet]. 2020 Jul 23;383(4):303–5. Available from: http://dx.doi.org/10.1056/NEJMp2016822

27. Murdock CC, Evans MV, McClanahan TD, Miazgowicz KL, Tesla B. Fine-scale variation in microclimate across an urban landscape shapes variation in mosquito population dynamics and the potential of Aedes albopictus to transmit arboviral disease. PLoS Negl Trop Dis [Internet]. 2017 May;11(5):e0005640. Available from: http://dx.doi.org/10.1371/journal.pntd.0005640

28. Caminade C, Turner J, Metelmann S, Hesson JC, Blagrove MSC, Solomon T, et al. Global risk model for vector-borne transmission of Zika virus reveals the role of El Niño 2015. Proc Natl Acad Sci U S A [Internet]. 2017 Jan 3;114(1):119–24. Available from: http://dx.doi.org/10.1073/pnas.1614303114

29. Upadhyay RK. Markers for global climate change and its impact on social, biological and ecological systems: A review. Am J Clim Change [Internet]. 2020;09(03):159–203. Available from: https://www.scirp.org/journal/doi.aspx?doi=10.4236/ajcc.2020.93012

30. Lloyd AL, Zhang J, Root AM. Stochasticity and heterogeneity in host-vector models. J R Soc Interface [Internet]. 2007 Oct 22;4(16):851–63. Available from: http://dx.doi.org/10.1098/rsif.2007.1064

31. Huber JH, Childs ML, Caldwell JM, Mordecai EA. Seasonal temperature variation influences climate suitability for dengue, chikungunya, and Zika transmission. PLoS Negl Trop Dis [Internet]. 2018 May;12(5):e0006451. Available from: http://dx.doi.org/10.1371/journal.pntd.0006451

32. Mordecai EA, Cohen JM, Evans MV, Gudapati P, Johnson LR, Lippi CA, et al. Detecting the impact of temperature on transmission of Zika, dengue, and chikungunya using mechanistic models. PLoS Negl Trop Dis [Internet]. 2017 Apr;11(4):e0005568. Available from: http://dx.doi.org/10.1371/journal.pntd.0005568

33. Otero M, Solari HG, Schweigmann N. A stochastic population dynamics model for Aedes aegypti: formulation and application to a city with temperate climate. Bull Math Biol [Internet]. 2006 Nov;68(8):1945–74. Available from: http://dx.doi.org/10.1007/s11538-006-9067-y

34. Otero M, Solari HG. Stochastic eco-epidemiological model of dengue disease transmission by Aedes aegypti mosquito. Math Biosci [Internet]. 2010 Jan;223(1):32–46. Available from: http://dx.doi.org/10.1016/j.mbs.2009.10.005

35. Subramanian R, Romeo-Aznar V, Ionides E, Codeço CT, Pascual M. Predicting re-emergence times of dengue epidemics at low reproductive numbers: DENV1 in Rio de Janeiro, 1986–1990. J R Soc Interface [Internet]. 2020 Jun 24;17(167):20200273. Available from: https://doi.org/10.1098/rsif.2020.0273

36. Telle O, Nikolay B, Kumar V, Benkimoun S, Pal R, Nagpal BN, et al. Social and environmental risk factors for dengue in Delhi city: A retrospective study. PLoS Negl Trop Dis [Internet]. 2021 Feb;15(2):e0009024. Available from: http://dx.doi.org/10.1371/journal.pntd.0009024

37. Calado DC, Navarro-Silva MA. Influência da temperatura sobre a longevidade, fecundidade e atividade hematofágica de Aedes (Stegomyia) albopictus Skuse, 1894 (Diptera, Culicidae) sob condições de laboratório. Rev Bras Entomol [Internet]. 2002 [cited 2023 Mar 31];46(1):93–8. Available from: https://www.scielo.br/j/rbent/a/XVBztyQMQNy57qqNB4PB6xQ/?format=html

38. Lardeux FJ, Tejerina RH, Quispe V, Chavez TK. A physiological time analysis of the duration of the gonotrophic cycle of Anopheles pseudopunctipennis and its implications for malaria transmission in Bolivia. Malar J [Internet]. 2008 Jul 26;7:141. Available from: http://dx.doi.org/10.1186/1475-2875-7-141

39. Yang HM, Macoris MLG, Galvani KC, Andrighetti MTM, Wanderley DMV. Assessing the effects of temperature on the population of Aedes aegypti, the vector of dengue. Epidemiol Infect [Internet]. 2009 Aug;137(8):1188–202. Available from: http://dx.doi.org/10.1017/S0950268809002040

40. Beserra EB, Fernandes CRM, Silva SA de O, Silva LA da, Santos JW dos. Efeitos da temperatura no ciclo de vida, exigências térmicas e estimativas do número de gerações anuais de Aedes aegypti (Diptera, Culicidae). Iheringia, Sér Zool [Internet]. 2009 Jun

[cited 2023 Mar 31];99(2):142–8. Available from: https://www.scielo.br/j/isz/a/xrWcVLDyrm9dBMKP4JJXXkN/?format=html

41. Westbrook CJ. Larval ecology and adult vector competence of invasive mosquitoes Aedes albopictus and Aedes aegypti for Chikungunya virus [Internet]. search.proquest.com; 2010. Available from: https://search.proquest.com/openview/a26a089334286abf56e9a5062e12a95b/1?pq-origsite=gscholar&cbl=18750

42. Rueda LM, Patel KJ, Axtell RC, Stinner RE. Temperature-dependent development and survival rates of Culex quinquefasciatus and Aedes aegypti (Diptera: Culicidae). J Med Entomol [Internet]. 1990 Sep;27(5):892–8. Available from: http://dx.doi.org/10.1093/jmedent/27.5.892

43. Tun-Lin W, Burkot TR, Kay BH. Effects of temperature and larval diet on development rates and survival of the dengue vector Aedes aegypti in north Queensland, Australia. Med Vet Entomol [Internet]. 2000 Mar;14(1):31–7. Available from: http://dx.doi.org/10.1046/j.1365-2915.2000.00207.x

44. Kamimura K, Matsuse IT, Takahashi H, Komukai J, Fukuda T, Suzuki K, et al. Effect of temperature on the development of Aedes aegypti and Aedes albopictus. Medical entomology and zoology [Internet]. 2002;53(1):53–8. Available from: https://www.jstage.jst.go.jp/article/mez/53/1/53_KJ00000825540/_article/-char/ja/

45. Eisen L, Monaghan AJ, Lozano-Fuentes S, Steinhoff DF, Hayden MH, Bieringer PE. The impact of temperature on the bionomics of Aedes (Stegomyia) aegypti, with special reference to the cool geographic range margins. J Med Entomol [Internet]. 2014 May;51(3):496–516. Available from: http://dx.doi.org/10.1603/me13214

46. Lambrechts L, Paaijmans KP, Fansiri T, Carrington LB, Kramer LD, Thomas MB, et al. Impact of daily temperature fluctuations on dengue virus transmission by Aedes aegypti. Proc Natl Acad Sci U S A [Internet]. 2011 May 3;108(18):7460–5. Available from: http://dx.doi.org/10.1073/pnas.1101377108

47. Watts DM, Burke DS, Harrison BA, Whitmire RE, Nisalak A. Effect of temperature on the vector efficiency of Aedes aegypti for dengue 2 virus. Am J Trop Med Hyg [Internet]. 1987 Jan;36(1):143–52. Available from: http://dx.doi.org/10.4269/ajtmh.1987.36.143

48. Alto BW, Bettinardi D. Temperature and dengue virus infection in mosquitoes: independent effects on the immature and adult stages. Am J Trop Med Hyg [Internet]. 2013 Mar;88(3):497–505. Available from: http://dx.doi.org/10.4269/ajtmh.12-0421

49. Carrington LB, Armijos MV, Lambrechts L, Scott TW. Fluctuations at a low mean temperature accelerate dengue virus transmission by Aedes aegypti. PLoS Negl Trop Dis [Internet]. 2013 Apr 25;7(4):e2190. Available from: http://dx.doi.org/10.1371/journal.pntd.0002190

Fig. S1. Model parameters (eq. 5) as a function of temperature. The black circles represent experimental data (from (32) Supp Material), the red dots the mean value (with respect to temperature) and the dashed red lines the curves used as a model to describe the parameters variation. **A** biting rate (data values from (37,38)). **B** Number of eggs laid per female per day (data from (39,40)), **C** probability of mosquito egg-to-adult survival (data from (41–45)). **D** Probability of virus transmission from a bite of an infected mosquito to a susceptible human . **E** Probability of a susceptible mosquito to get the virus following a bite on an infectious human (D and E data are from (46–49)). The parameters of the curves shown in panels A, B and C are taken from (32) and those of panels D and E were determined in this article.

Fig S2. Percent of units at risk that belongs to the different socio-economics typologies as a function of $R0$* (threshold to classify spatial units at risk of dengue transmission when $R0$ is above this value). Pink triangles denote low socio-economic typologies, whereas black circles and gray dots represent medium and rich socio-economic conditions, respectively.

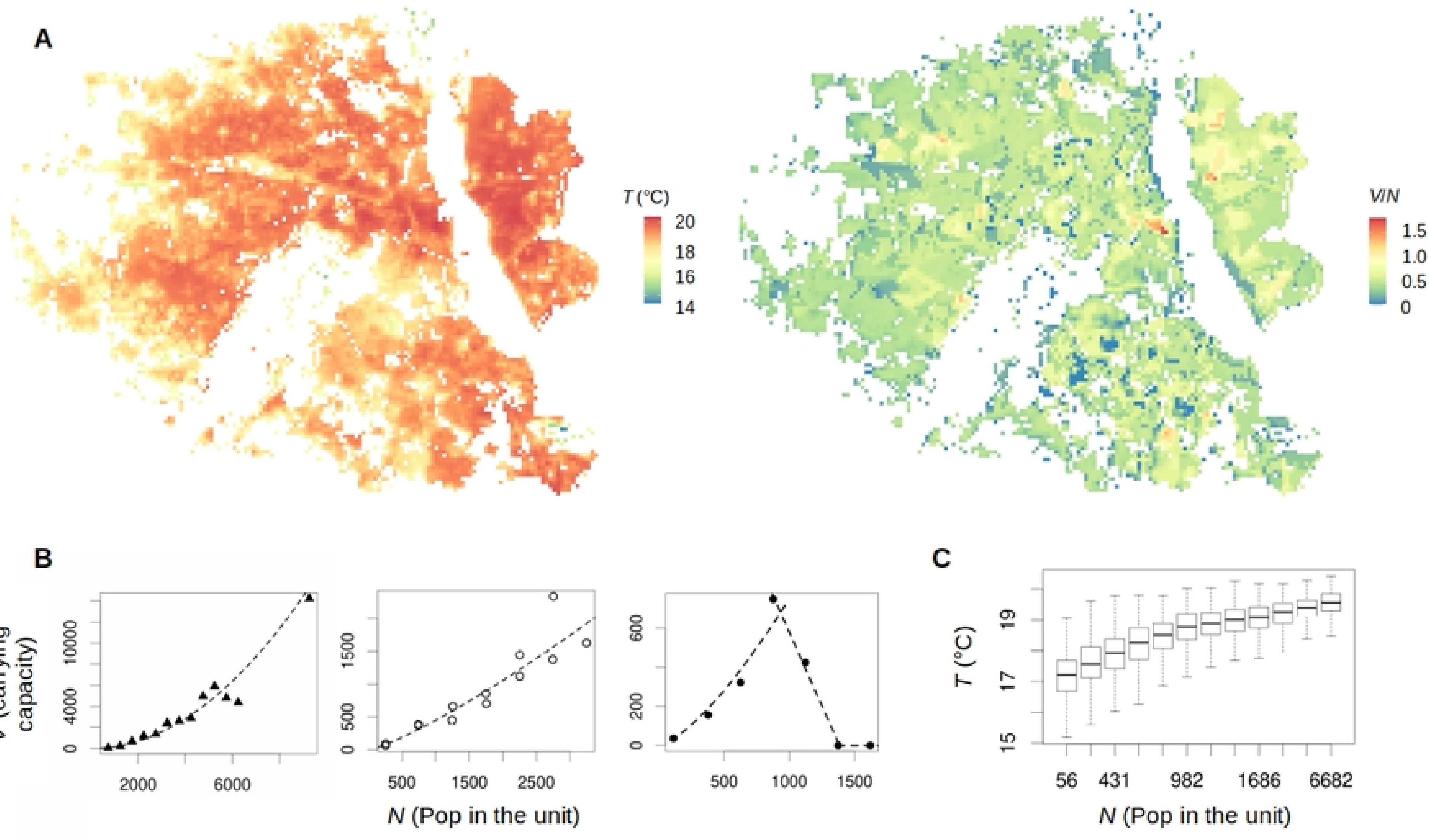

A
T (°C)
20
18
16
14
V/N
1.5
1.0
0.5
0
B
V (carrying capacity)
0
4000
10000
2000
6000
0
500
1500
500
1500
2500
N (Pop in the unit)
0
200
600
500
1000
1500
C
T (°C)
15
17
19
56
431
982
1686
6682
N (Pop in the unit)

Fig1

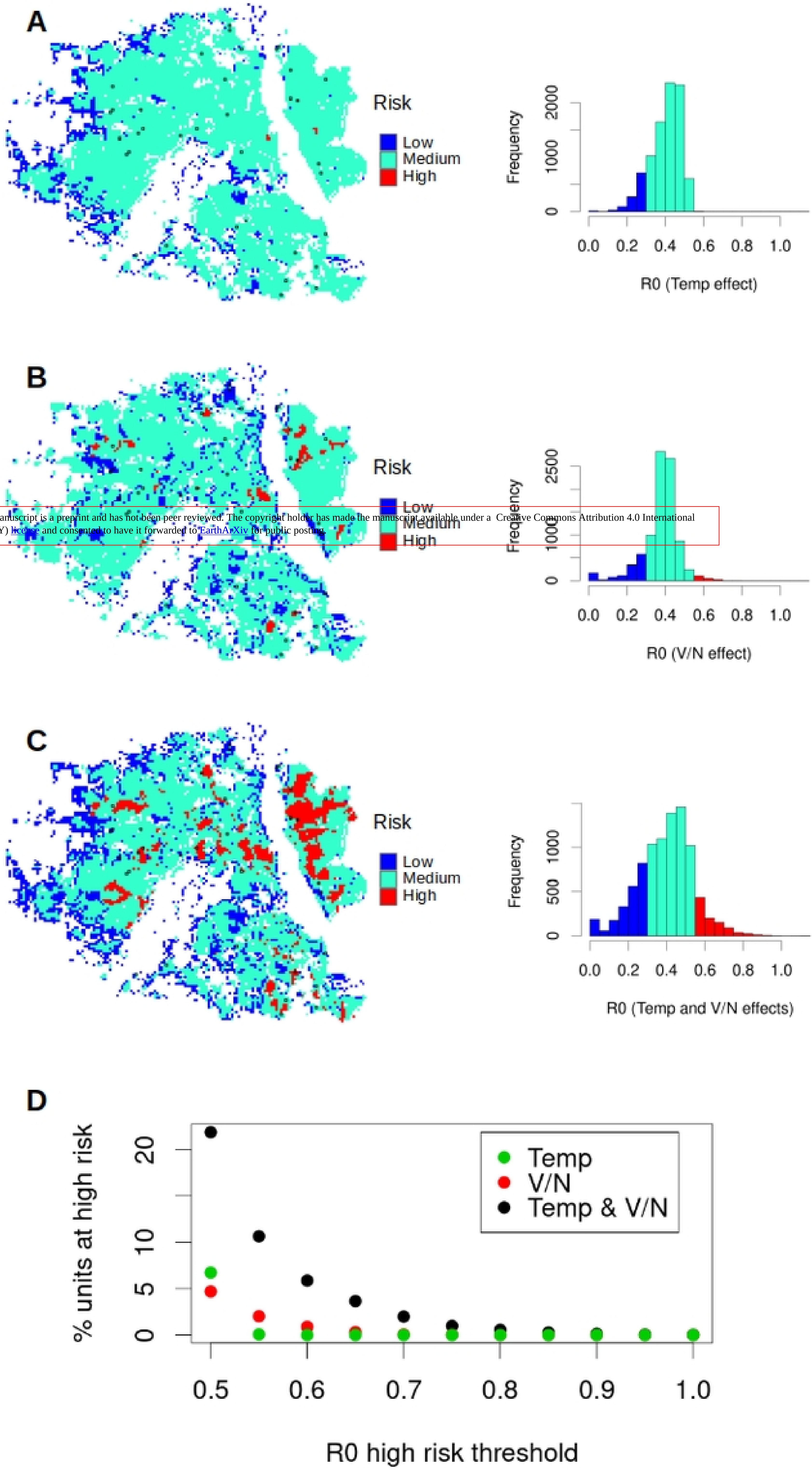
A
Risk
Low
Medium
High
Frequency
R0 (Temp effect)
B
Risk
Low
Medium
High
Frequency
R0 (V/N effect)
C
Risk
Low
Medium
High
Frequency
R0 (Temp and V/N effects)
D
% units at high risk
Temp
V/N
Temp & V/N
R0 high risk threshold

Figure

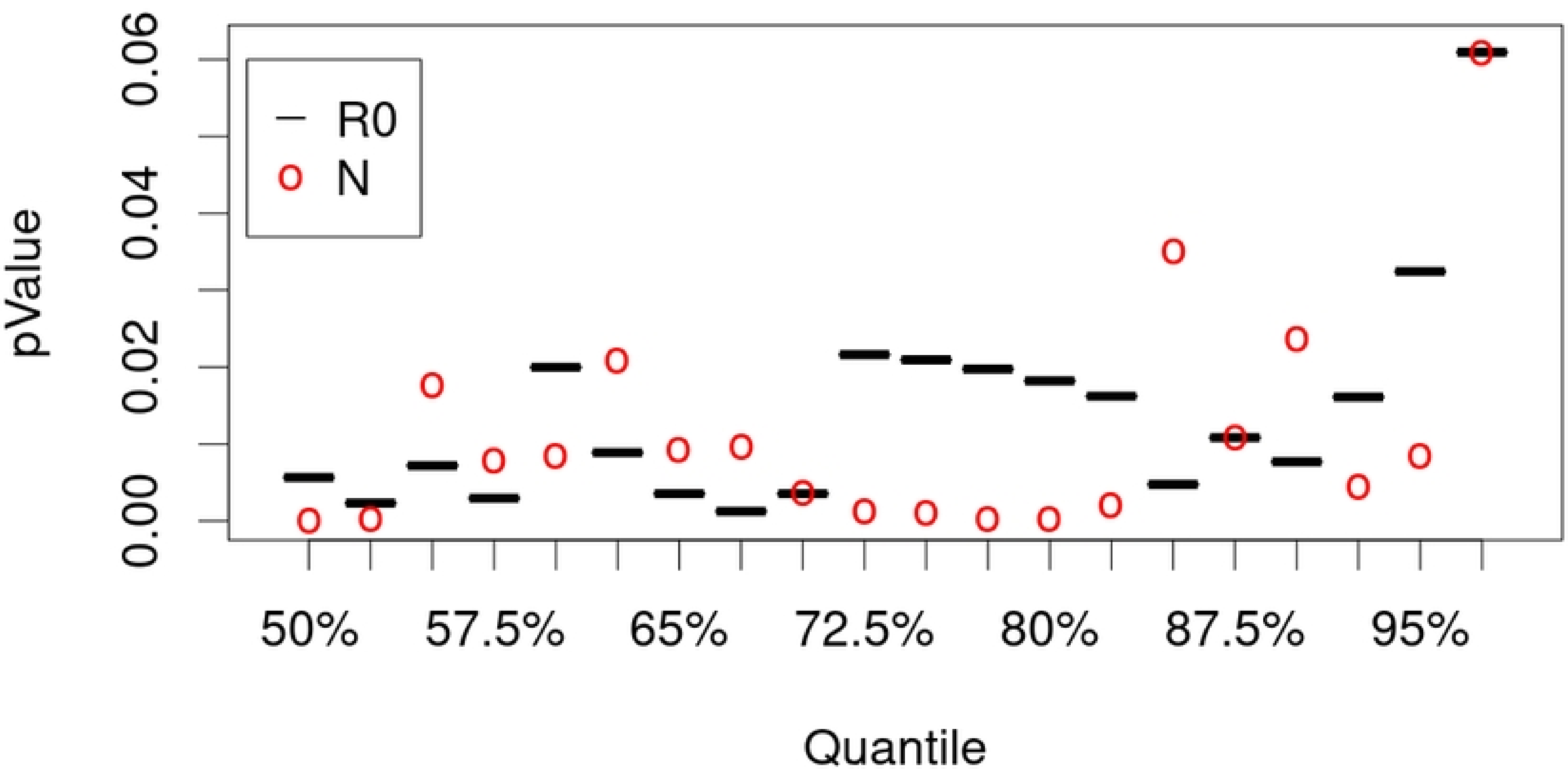

Figure

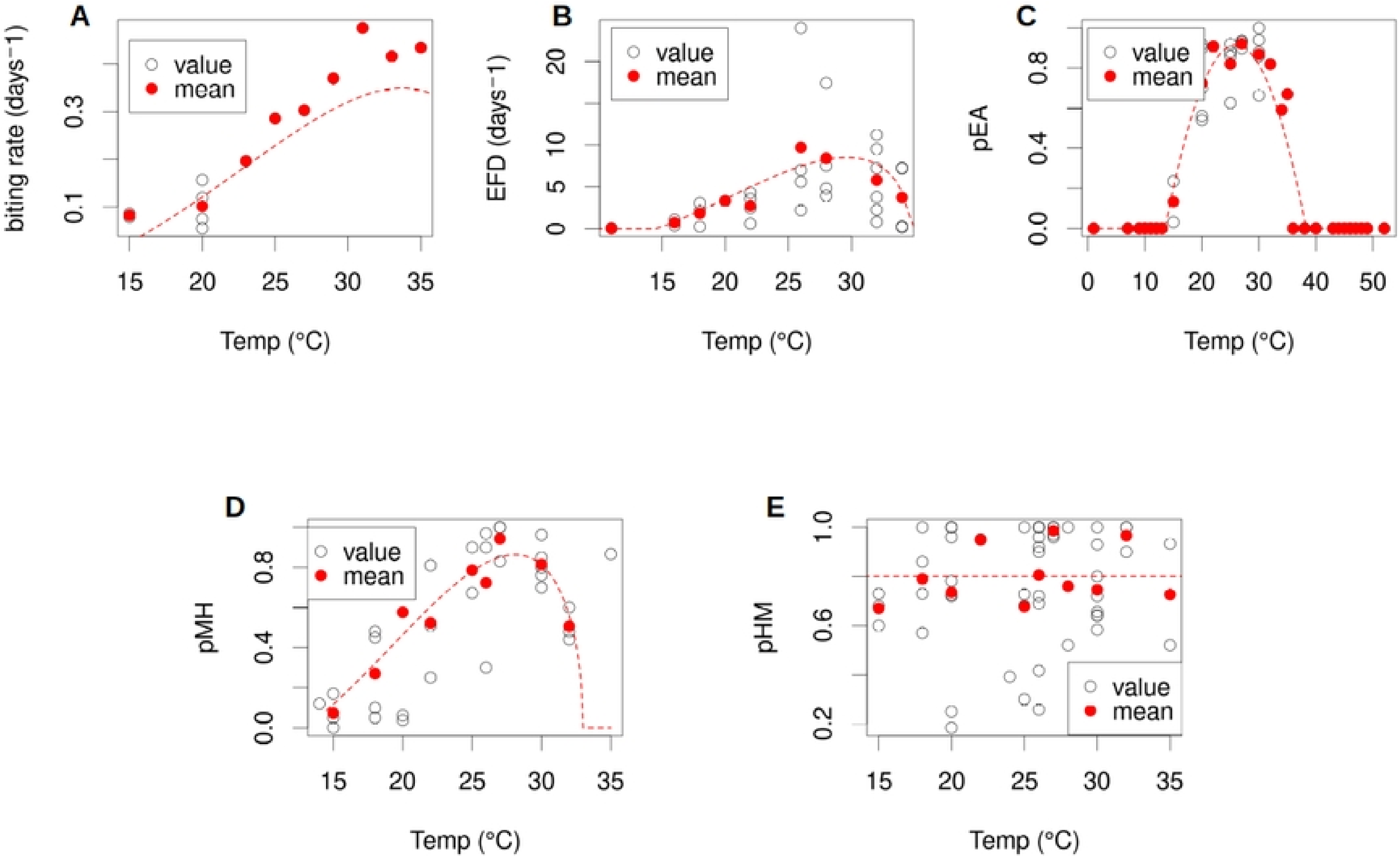

Figure supporitng information

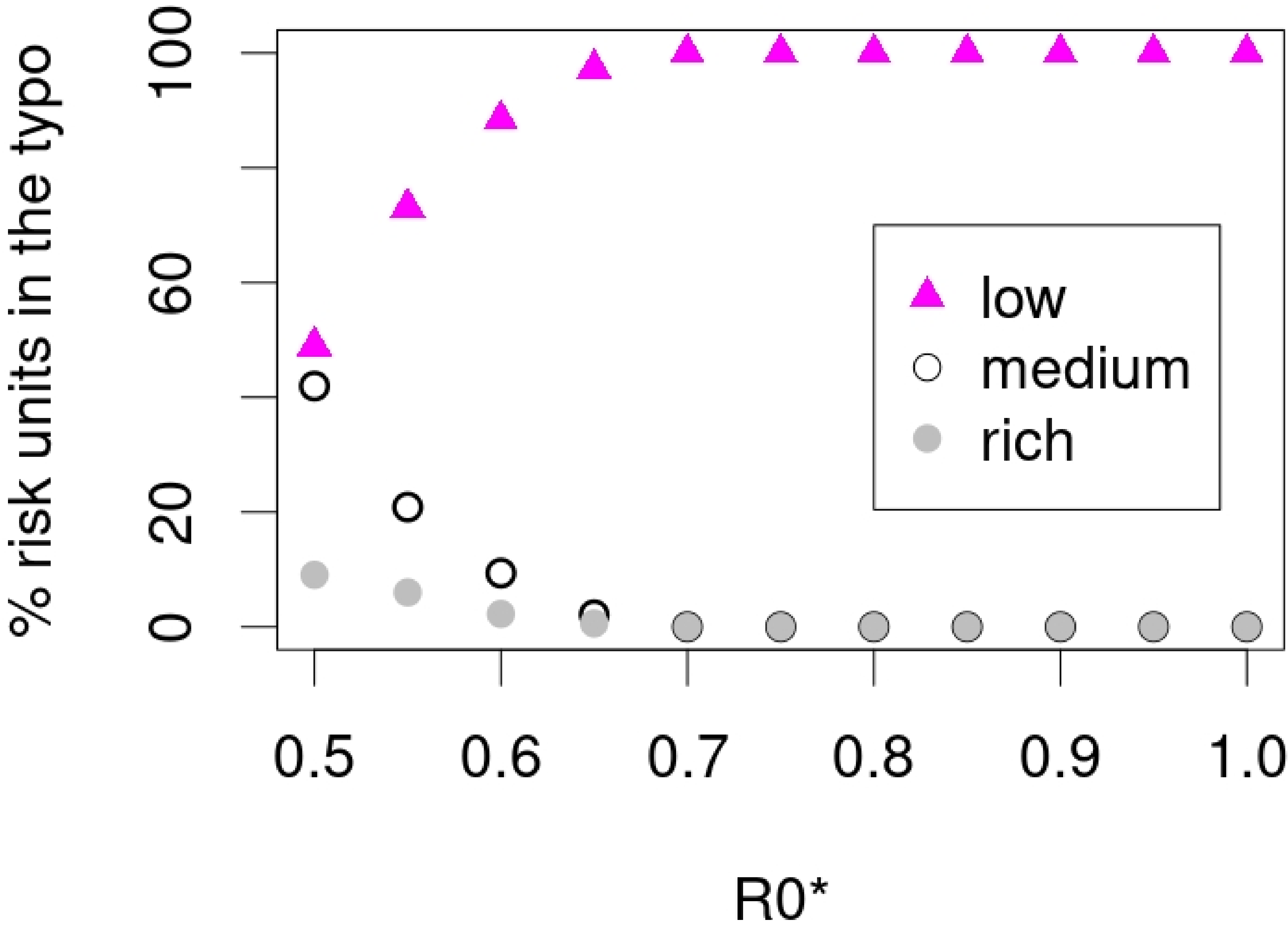

Figure supporitng information